Cantilever-based *in vivo* measurements in the early *Drosophila* embryo reveal adiabatic elastic response on developmentally relevant time scales

Mohamad Ibrahim Cheikh[1], Joel Tchoufag[2], Kevin Dean[3], Swayamdipta Bhaduri[1], Zhang Chuzhong[4], Kranthi Kiran Mandadapu[2], and Konstantin Doubrovinski[1]*

Abstract

Understanding physical mechanisms underlying morphogenesis requires the knowledge of the mechanical properties of embryonic tissue. Despite a long-standing interest in this subject, very few *in vivo* measurements are currently available. Here, using the early fly embryo as a model, we describe a novel cantilever-based technique for measuring material properties of embryonic tissues. A major advantage of our approach is the ability to exert large (nanonewton-range) forces with subcellular spatial precision: our technique improves signal to noise by approximately an order of magnitude compared to previous methods. This advance allowed us to demonstrate that deformation caused by force applied to a single cell edge spreads across the whole embryo on a time scale of seconds and that the mechanical response is dominated by system-size effects, and not friction between the tissue and its environment. Based on these measurements, we estimate the Young's modulus of the cellular edges in the early embryo.

Introduction

A predictive understanding of tissue morphogenesis requires knowing the material properties of embryonic tissues. To meet this demand, a number of techniques for probing material properties of cells have recently been developed, and have been reviewed elsewhere (Wu et al. 2018). However, these methods have several shortcomings. Optical and magnetic tweezers typically generate forces in the piconewton range, such that the resulting displacements do not exceed a few microns. Additionally, those forces are usually applied on a time-scale of seconds. Hence, the force- and time-scales in these measurements tend to be well below the scales characteristic of morphogenesis (which typically unfolds on a time-scale of tens of minutes or hours and results in deformations on the order of tens to hundreds of microns). Since material properties are in general expected to vary depending on the time- and force-scales involved, such measurements may not be relevant for understanding the physical mechanisms underlying morphogenesis. Bendable cantilevers and biological atomic force microscopes (AFM) allow for applying much larger forces over larger times. However, these techniques are hard to use in living embryos since introducing a probe into an embryo without significantly disrupting the tissue proves challenging. Recently, we and one other lab introduced a measurement technique based on the use of ferrofluid droplets (Doubrovinski et al. 2017, Serwane et al. 2016). This method allows probing tissue with forces on the order of tens of nanonewtons, but requires a probe that is fairly large (10-20 microns; several-fold larger than a typical cell), thus possibly locally damaging the tissue that is being probed.

To address the shortcomings of the currently available methods, here, we introduce a novel measurement technique based on soft bendable polymer-based cantilevers that may be introduced into an embryo to probe tissue mechanics with high spatial precision. Based on our measurements, using an essentially parameter-free model we demonstrate that the response of the tissue is completely dominated by system-size effects. In particular, pulling force applied to a single cell edge results in deformation that propagates throughout the entire embryo in seconds. Additionally, viscous friction between the tissue and its environment is largely

[1] Department of Biophysics, University of Texas Southwestern Medical Center, Dallas, TX 75390-9050.
[2] Department of Chemical and Biomolecular Engineering, University of California, Berkeley, CA 94720, USA., Chemical Sciences Division, Lawrence Berkeley National Laboratory, Berkeley, CA 94720, USA.
[3] Department of Bioinformatics, University of Texas Southwestern Medical Center, Dallas, TX 75390-9050.
[4] Department of Material Science and Engineering, University of Texas at Arlington, Arlington, TX 76019-0031
* correspondence to: Konstantin.Doubrovinski@UTSouthwestern.edu

irrelevant. Finally, our measurements allowed us to place an upper bound on the Young's modulus of a cellular edge.

Results

Progress towards establishing the mechanical properties of animal tissue is largely limited by both the availability of measurements as well the development of quantitative models that can realistically account for both the material properties and the geometry of cells. To tackle the first challenge, we developed a novel technique which is largely inspired by previous measurements on tissue culture cells where a bendable cantilever of glass was used as a force probe (Desprat et al. 2005). Our probe consists of a long stiff glass pipette with a soft polymer tip that acts as a flexible cantilever. The deflection of the cantilever is used to quantify the force applied by the tip; in combination with the resulting tissue deformation, a force-displacement relationship can be established.

If a bendable cantilever is used to probe the mechanics of *Drosophila* embryonic cells, one is confronted with several inherent technical challenges. First, it is necessary to introduce the probe without severely perturbing the tissue being probed. Before introducing our probe into an embryo, we use a pulled glass pipette to cut a slit in the embryo on the opposite surface from which we plan to take measurements, then insert the probe through this cut. Quite strikingly, we found that when a fly embryo is cut along one side, the side that is not cut continues to develop completely normally showing no noticeable defects. In particular, if a cut is made on the dorsal side during the early stage of cellularization, on the opposite uncut side, cellularization completes and is followed by ventral furrow formation and germ band extension. Thus, we conclude that this method is (relatively) noninvasive and is unlikely to significantly perturb the properties of the tissue that is being probed.

Another technical challenge is making the cantilever sufficiently compliant to appreciably bend under the relevant nanonewton-range forces. In previous work where cantilevers were used to probe the mechanics of e.g. tissue culture cells and spindles, probes of glass were used (Desprat et al. 2005, Shimamoto Y and Kapoor 2012). Typically, in those experiments, maximal cantilever deformations were smaller than a micron, or a few microns at most. Deflections this small are readily quantifiable if the cantilever is immersed in an optically transparent environment (such as tissue culture medium) and imaged in bright field. This is however hard to achieve when doing measurements in the rather opaque embryo interior. Our solution is to make a shorter cantilever using material that is much more compliant than glass. Specifically, our cantilevers are micro-fabricated from PDMS (polydimethylsiloxane; see methods section). In brief, a standard injection glass pipette is used as a mold for making a PDMS cantilever. The tip of a glass pipette is filled with PDMS by letting the uncured mixture of polymer and crosslinker enter the capillary through an opening at the tip by capillary action. After the polymer is cured, the glass scaffold is etched away in a solution of hydrofluoric acid to expose the soft PDMS core.

Another challenge is visualizing the PDMS cantilever within the rather opaque embryonic interior. To this end, we make cantilevers brightly fluorescent by introducing a dye into the polymer. In our experience, hydrophilic dyes don't mix with PDMS, whereas many hydrophobic dyes prevent its curing. We found that a green variant of BODIPY (boron-dipyrromethene) dye mixes well with PDMS and does not interfere with the curing process. In this way, our cantilever probes are made fluorescent and are readily visualized within the embryo (Figs. 1,3).

Finally, to probe tissue mechanics by subjecting cells to a pulling force, it is necessary to attach the cantilever to a cell that is being probed. Here, we capitalize on an unusual feature of fly development. Through the earliest several cycles of mitosis, the *Drosophila* embryo is a syncytium, i.e. a very large cell with multiple nuclei sharing common cytoplasm. Subsequently, in the process of cellularization, membranes extend from the surface of the embryo and protrude between the nuclei, such that the cytoplasm is for the first time partitioned into individual cells. During cellularization, every newly forming cell is in effect open on its basal side, such that the interior of that cell is connected to the yolk compartment residing in the center of the embryo (see Fig. 1a for a schematic illustration). This allows us to insert the cantilever through the basal hole. As the cantilever is translated parallel to the cellular layer, it pushes against the adjacent cell edge, thus exerting a pulling force on

that cell. Cantilever movement is controlled using a piezo-actuator mounted on the microscope stage (see Fig. 1, and the Methods section).

A typical measurement is shown in Fig. 3 (see also Supplemental movie 1). The cantilever is inserted through an incision on the ventral side of the embryo, allowing dorsal cells to be probed. To visualize cellular deformations arising from the applied force, cellular membranes were stained with a bright fluorescent dye (CellMask Deep Red) injected into the perivitelline space prior to a measurement. We found dye injections necessary when imaging the midsagittal plane using confocal laser scanning microscopy, since the signal from fluorescent protein-based membrane markers proved insufficient. After the cantilever is inserted into a cell, the base of the cantilever is translated 30 microns parallel to the cellular layer for 60 seconds; it is then held in place for 60 seconds, after which it is retracted from the interior of the cell to allow the cellular layer to relax. When pulled in this way, the cellular layer substantially deforms. At the same time, the cantilever undergoes substantial bending that is readily quantified from the acquired images.

To determine tissue material properties from the data such as that shown in Figure 3, it is necessary to calibrate the probe; in other words, the force-deflection relation of the cantilevers need be measured. To this end, we used three complementary techniques: (1) fabricating a macroscopic rod of PDMS to measure its deformation under its own weight (Fig. S2), (2) pulling the cantilever through a fluid of known viscosity to measure the resulting deflection (Fig. 2a-c), and (3) probing the cantilever with an AFM probe (Fig. 2d,e). The details of these measurements are deferred to the Methods section. The three methods estimate the Young's modulus of the PDMS comprising the cantilever to be 1.6 MPa, 1.2 MPa and 2 MPa respectively.

Measurement results are presented as a kymograph (Fig. 4a,b). In this figure, the horizontal direction corresponds to time (increasing towards the left), while the vertical direction corresponds to the position along a section through the embryonic epithelium. The purple signal indicates the location of individual membranes. The green trace is the position of the cantilever. To better quantify the time-course of the deformation, we plotted the profiles of tissue displacement corresponding to several time-points during the loading and the holding phases. Schematic Fig. 4c illustrates how tissue deformation profiles are constructed from a recorded kymograph. Instantaneous positions of individual membranes are readily obtained by computationally tracking magenta traces in Fig. 4a. Graphs shown in Figs 4d,e are obtained by plotting the displacement of the individual tracked membranes as a function of their initial position along the mid-section through the epithelium. Measurements performed on different specimen are highly consistent as shown in Fig. S4.

To interpret our measurements, we start by considering a minimal model where an elastic sheet, subjected to viscous drag, is stretched by a concentrated force. Initially, we assume that boundaries of the sheet are "far off at infinity" and do not significantly influence the dynamics. In what follows, we call this the "drag-dominated" model. In this limit, the profile of the deformation (i.e. curves in Figs. 4d,e) takes the general form $u_x(x,t) = t^{\alpha} g(x/t^{\beta})$; for details see (Doubrovinski et al. 2017), in particular, Fig. S4 therein. That is, deformation profiles at different times are invariant up to re-scaling the y- and the x-axis by the factors t^{α} and t^{β} respectively. It may further be shown that if the sheet is linearly elastic and if friction has some fixed magnitude per unit area, then, β=$1/2$ (Doubrovinski et al. 2017). If, instead, the elastic sheet is a floppy network of hexagons with linearly elastic edges, $\beta = 3/8$ (Doubrovinski et al. 2017). If a two-dimensional linearly elastic sheet is in contact with a semi-infinite three-dimensional fluid domain, β increases to $\beta = 1$. Our measurements, however, do not align with these predictions. Fig. 4d' shows that deformation profiles at different times can be collapsed on almost the same master curve without re-scaling the x-axis. Hence, β must assume a small value well below $1/2$ and the drag-dominated model must be rejected. Instead, our data are consistent with a situation where the external force on the sheet is balanced by forces acting on its fixed boundaries. Thus, the dynamics are dominated by system-size effects and the deformation propagates throughout the whole embryo on a timescale of seconds. This interpretation raises a question -- how can dynamics be governed by boundary effects if the embryo is an ellipsoid and, thus, appears to not have boundaries? An explanation is suggested in the schematic Fig. 4f. Consider a prolate ellipsoid whose surface is an elastic shell. Assume further that points on the ellipsoid surface are constrained to remain on the surface. If a concentrated force stretches the surface parallel to the long (major) axis of the ellipsoid, the deformation cannot be compensated by subsequent rigid

rotation of the whole ellipsoid. Thus the ellipsoid's minor axis shown in Fig. 4f must stretch. In this way, the geometry of the ellipsoid gives rise to system size “boundary” effects even though the surface is closed.

To further test if the dynamics are dominated by system-size effects, we considered time-dependence of the applied force as measured from cantilever deflection. Fig. 6a shows that the force on the cantilever increases linearly in the loading phase and then drops off to approximately half its original magnitude during the holding phase. To interpret this observation, consider first a situation where the external force on the deforming tissue is balanced by viscous drag and where the boundary effects are negligible. In this case, once the pulling stops, the tissue in the vicinity of the point being pulled will ultimately relax completely and the measured force will drop to zero. However, if the boundaries of the tissue are held fixed sufficiently close to the point being pulled, complete relaxation of the tissue will be prevented. Hence, in the latter case, the force will asymptote to a non-zero value, as seen in measurements. Note that tissue relaxation is not prevented by mechanical contact with a fixed boundary, but due to mechanical contact with the tissue on the side of the embryo opposite to the side being pulled (schematic Fig. 4f). Additionally, we find that the tissue remains stretched and does not deform at all after pulling (Fig. 4d’’). This further confirms our interpretation.

It is also of interest to note that the force measured from cantilever deflection does not change abruptly when the loading stops (whereafter the tissue is held fixed in a deformed state). This observation strongly suggests that embryonic tissue does not exhibit appreciable viscous shear stress if a deformation takes place on a developmentally relevant time scale of minutes. Specifically, since viscous shear stress is directly proportional to shear rate, it must experience an abrupt decrease when the motion stops at the end of the loading phase. Since no discontinuous change in the force is seen (Fig. 6a), viscous shear stress is likely negligible. Note that this does not imply that the cytoskeleton does not contribute to the dissipation through other mechanisms. For example, stresses may still be dissipated through the turnover of the elastic constituents (actin). In fact, the measured force dynamics suggest that this is a likely interpretation, since the force does indeed relax by approx. 50 percent following loading.

Having established that the dynamics are dominated by system-size effects, we considered the physical nature of the observed tissue recoil. To study the recoil dynamics, we developed a computational model of the early blastula. The details of our numerical treatment are deferred to the Supplementary section; all code is publicly available under https://github.com/doubrovinskilab/cantilever_embryo_rheology. In brief, cells are prisms whose surface edges are linearly elastic shells, see Fig. 5a-d. The interior of a cell is filled with cytoplasm, modeled as Newtonian fluid whose viscosity is set to the previously measured value of 1000 cP (Doubrovinski et al. 2017, Selvaggi et al. 2018). Embryo surface is a rigid shell (vitelline membrane) where no-slip condition is imposed. The small gap between the vitelline membrane and the cellular layer is filled with Newtonian fluid (perivitelline fluid) having viscosity of water. External force is applied to a single cell edge, representing the effect of the cantilever. Geometries of all the relevant structures were taken from measurements. Comparing the simulated tissue deformation profile to the corresponding measurement, we see that the model closely captures the measured data, at least as long as the imposed deformation is small, see Fig. 4e (see also Supplemental movie 2). Figs. 5e,f shows that maximal (simulated) force on the cantilever increases linearly with the Young’s modulus E of the cellular edges, whereas the characteristic time of the recoil decreases. Importantly, if E is chosen sufficiently high to match the maximal value of the applied force, the predicted time of recoil appears at least an order of magnitude larger than observed. This result can be accommodated by assuming that the force on the cantilever is completely dominated by the basal portion of the cells, whereas stresses in the apical and lateral domains are significantly smaller. This conclusion is important to understanding the dynamics of gastrulation since tissue deformation during the gastrulation phase involves mainly the apical and the lateral cellular domains. To confirm this conclusion through independent measurements, we conducted experiments using a previously developed assay, where the force is applied to cells using a ferrofluid droplet (Figs. 6b,c; see Doubrovinski et al. 2017). Occasionally, it is possible to generate a ferrofluid droplet that is sufficiently small to enter the interior of a cell through the basal hole. This trick allowed us to exert pulling force on the lateral cellular domain without a direct contact between the basal side and the droplet. Measurement results appear very different depending on whether or not the droplet makes contact with the basal side (see Supplemental movie 3). In the latter case, the droplet exhibits rapid displacement without slowing down (compare Figs. 6c and Fig. 1d in Doubrovinski et al. 2017; Supplemental

movie 3). Therefore, the response is dominated by the basal domain which agrees with the observations in e.g. (Sokac and Wieschaus 2008), showing that actin is particularly prominent on the basal membranes.

Finally, based on our simulations, one can obtain an estimate of the elastic modulus of cellular edges, E. We found that the time-scale of the recoil would be significantly underestimated unless E is set lower than 0.05 nN/μm. Two assumptions are essential to this analysis. (1) Shear stresses are only present in the cytoplasm and not in the membrane-associated cytoskeleton and (2) elastic stresses don't dissipate on the time scale of tissue relaxation. Assumption (1) was justified above based on the observation that force does not change abruptly after the cantilever stops translating. Our force measurements imply that assumption (2) can only hold if the tissue recoil requires much less than 1 min. But since this indeed would be the case for a large enough E, those values of E may in fact be rejected.

Conclusions

In this work, we have introduced a novel measurement technique that enables one to apply concentrated force to a single epithelial cell in a living developing embryo. We envisage that our method, being simple and cost effective, will find applications in many other systems.

Using our method, we have been able to demonstrate that mechanical response of the tissue on time scales comparable to the time scale on which morphogenesis proceeds are dominated by system size effects. It is important to note that this conclusion is entirely independent of the magnitude of the applied force or the magnitude of the final tissue deformation: relevant is only the time scale of the loading. Any deformation, however small, will propagate through the tissue on a timescale of seconds. Note additionally that any model used to estimate the mechanical properties of the tissue must take this into account. This was not realized in the previous related work (Doubrovinski et al. 2017, Bambardekar et al. 2015, D'Angelo et al. 2019).

Finally, we show that the mechanical properties are non-uniform along the apico-basal axis of blastocyte cells. Specifically, the basal domain is far more rigid than the lateral and apical cellular edges.

It is of particular interest to compare our results with the previous work on the system. In an important recent publication (D'Angelo et al. 2019), authors performed magneto-rheology on *Drosophila* blastula using 5 μm magnetic beads. To interpret their measurements, the authors proposed a model where the external force on the tissue is balanced by viscous drag from its environment. Our data suggest a different interpretation: the force is balanced by system-size ("boundary") effects, while viscous drag is unimportant. The difference between the work in (D'Angelo et al. 2019) and ours is that cantilever-based perturbation generates considerably larger deformations such that the spatial propagation of the deformation can be quantified well away from the site of force application. Additionally, our method of labeling cells with CellMask dye further enhances the ability to quantify small deformations. Furthermore, in (D'Angelo et al. 2019) it was suggested that the tissue softens during the course of cellularization. We propose an alternative interpretation. During the early stage of cellularization, cells are short and magnetic bead is in mechanical contact with the very rigid basal side. At a later stage in cellularization, cells become taller and the bead only contacts the apical and/or the lateral cellular domains which are much softer. In (D'Angelo et al. 2019) it was noted that colcemid treatment caused the tissue to not soften. This is consistent with our suggestion: microtubule depolymerization stops cellularization such that cells remain short (Royou et al. 2004). In this way, differences in the (apparent) material properties reported in (D'Angelo et al. 2019) reflect differences in the material properties of the different cellular domains, and not changes due to the developmental progression.

Results presented here must be taken into account in any quantitative treatment aiming to model the dynamics of gastrulation in *Drosophila,* key model system used to study the biophysical mechanisms of morphogenesis. We further envisage the similar physical effects may be equally relevant to experiments in other model systems such as zebrafish (Behrndt et al. 2012) and *C. elegans* (Mayer et al. 2010).

References:

Bambardekar K., Clément R., Blanc O., Chardès C., and Lenne P-F. Direct laser manipulation reveals the mechanics of cell contacts in vivo. PNAS 112 (5) 1416-1421 (2015).

Behrndt, M., Salbreux, G., Campinho, P., Hauschild, R., Oswald, F., Roensch, J., Grill, S. W. and Heisenberg, C.-P. Forces driving epithelial spreading in zebrafish gastrulation. Science 338, 257 (2012).

D'Angelo A., Dierkes K., Carolis C., Salbreux G. and Solon J. *In vivo* Force Application Reveals a Fast Tissue Softening and External Friction Increase during Early Embryogenesis. Curr. Biol. 29(9) 1564-1571 (2019).

Desprat N., Richert A., Simeon J. and Asnacios A. Creep Function of a Single Living Cell. Biophys. J. 88 2224-2233 (2005).

Doubrovinski K., Swan m., Polyakov O., and Wieschaus E. Measurement of cortical elasticity in Drosophila melanogaster embryos using ferrofluids. PNAS 114 (5) 1051-1056 (2017).

Figard L., Xu H., Garcia H., Golding I., Sokac A. M. The Plasma Membrane Flattens Out to Fuel Cell-Surface Growth during Drosophila Cellularization. Dev. Cell 27 (6) 648-655 (2013).

Khalilgharibi N., Fouchard J., Asadipour N., Barrientos R., Duda M., Bonfanti A., Yonis A., Harris A., Mosaffa P., Fujita Y., Kabla A., Mao Y., Baum B., Muñoz J., Miodownik M. and Charras G. Stress relaxation in epithelial monolayers is controlled by the actomyosin cortex. Nat. Phys. 15, 839–84 (2019).

Mayer, M., Depken, M., Bois, J. S., Jülicher, F. and Grill, S. W. Anisotropies in cortical tension reveal the physical basis of polarizing cortical flows. Science 467, 617-621. (2010).

Royou A., Field C., Sisson J.C., Sullivan W., and Karess R. Reassessing the Role and Dynamics of Nonmuscle Myosin II during Furrow Formation in Early Drosophila Embryos. Mol. Biol. Cell 15, 838–850. (2004).

Selvaggi L., Pasakarnis L., Brunner D. and Aegerter C. M. Magnetic tweezers optimized to exert high forces over extended distances from the magnet in multicellular systems. Review of Scientific Instruments, 89(4):045106. (2018)

Serwane F., Mongera A., Rowghanian P., Kealhofer D., Lucio A., Hockenbery Z. and Campàs O. In vivo quantification of spatially varying mechanical properties in developing tissues. Nat. Methods 14(2) 181-189 (2016).

Seung H.S. and Nelson D.R. Defects in flexible membranes with crystalline order. Phys. Rev. A 38 1005–1018 (1988).

Shimamoto Y and Kapoor T. Microneedle-based analysis of the micromechanics of the metaphase spindle assembled in *Xenopus laevis* egg extracts. Nat. Protoc 7 (5) 959-969 (2012).

Sokac A.M., Wieschaus E. Zygotically controlled F-actin establishes cortical compartments to stabilize furrows during Drosophila cellularization. J. Cell. Sci. 121, 1815-1824. (2008)

Wiggins C., Riveline D., Ott A. and Goldstein R. Trapping and Wiggling: Elastohydrodynamics of Driven Microfilaments. Biophys. J. 74(2) 1043-1060 (1998).

Wu P.-H., Aroush D. R-B., Asnacios A., Chen W.-C., Dokukin M., Doss B., Durand ., Ekpenyong A., Guck J., Guz N., Janmey P., Lee J., Moore N., Ott A., Poh Y.-C., Robert Ros5, Sander M., Sokolov I., Staunton J., Wang J., Whyte G., and Wirtz D. Comparative study of cell mechanics methods. Nat. Methods 15(7) 491-498 (2018).

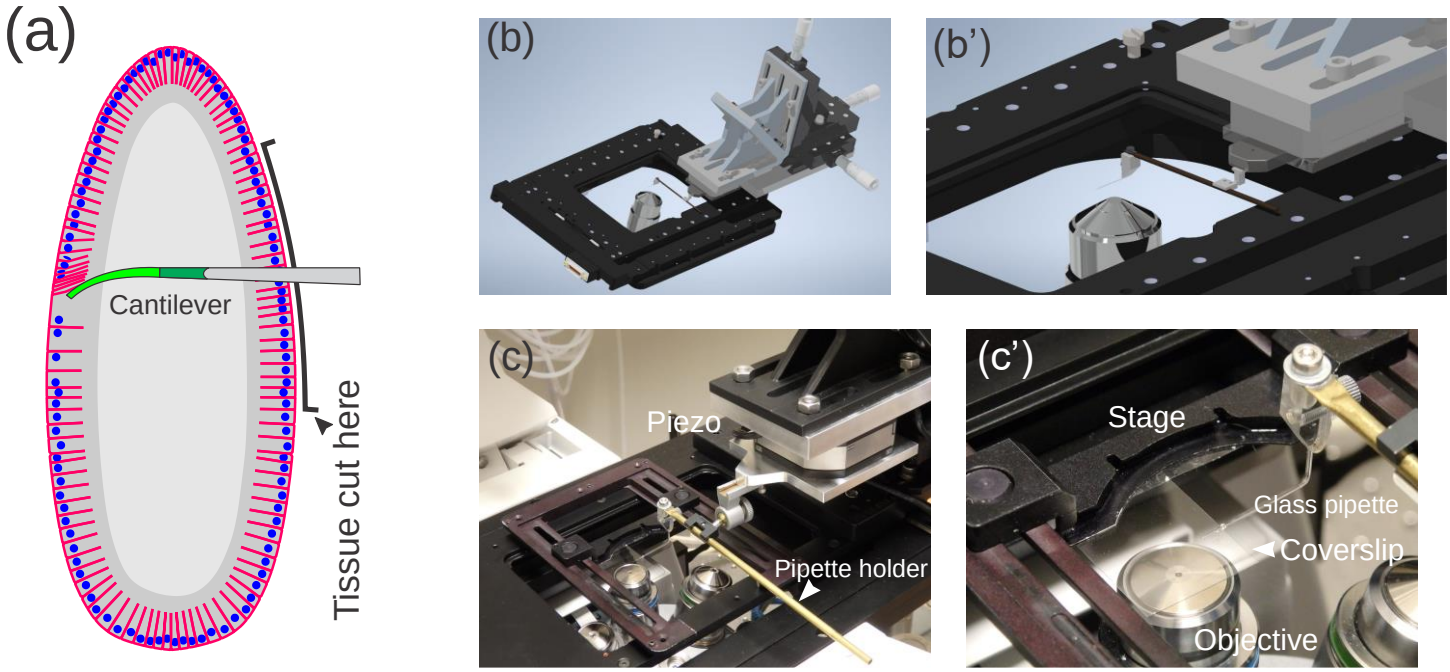

Figure 1. Schematic of the experiment and an illustration of the setup. Embryo is cut along one side. Cantilever mounted on at the end of a glass pipette is inserted through the cut. At the relevant developmental stage, cells have a “hole” on their basal side such that they are open to yolk sack. Cantilever is inserted into a cell through the basal hole and translated so as to deform the cellular layer. (b) A schematic of the setup. Three axis translation stage is mounted directly on the microscope stage to minimize vibrations. Two 45° angle brackets are used mount a piezo actuator on the translation stage. A pipette holder is connected to the piezo-actuator by means of a ball-and-joint mount providing additional degrees of freedom to more readily access the sample. A glass pipette housing the PDMS micro-cantilever is bent 90° to fit into the pipette holder, at the same time minimally obstructing access of the pipette tip to the specimen. (b’) Same as (a) zoomed in on the pipette holder. (c) A picture of the setup showing how a sample is mounted on a modified stage insert. The coverslip holding the embryos is attached to the insert using double-sided tape. (c’) Same as (c) zoomed in on the coverslip.

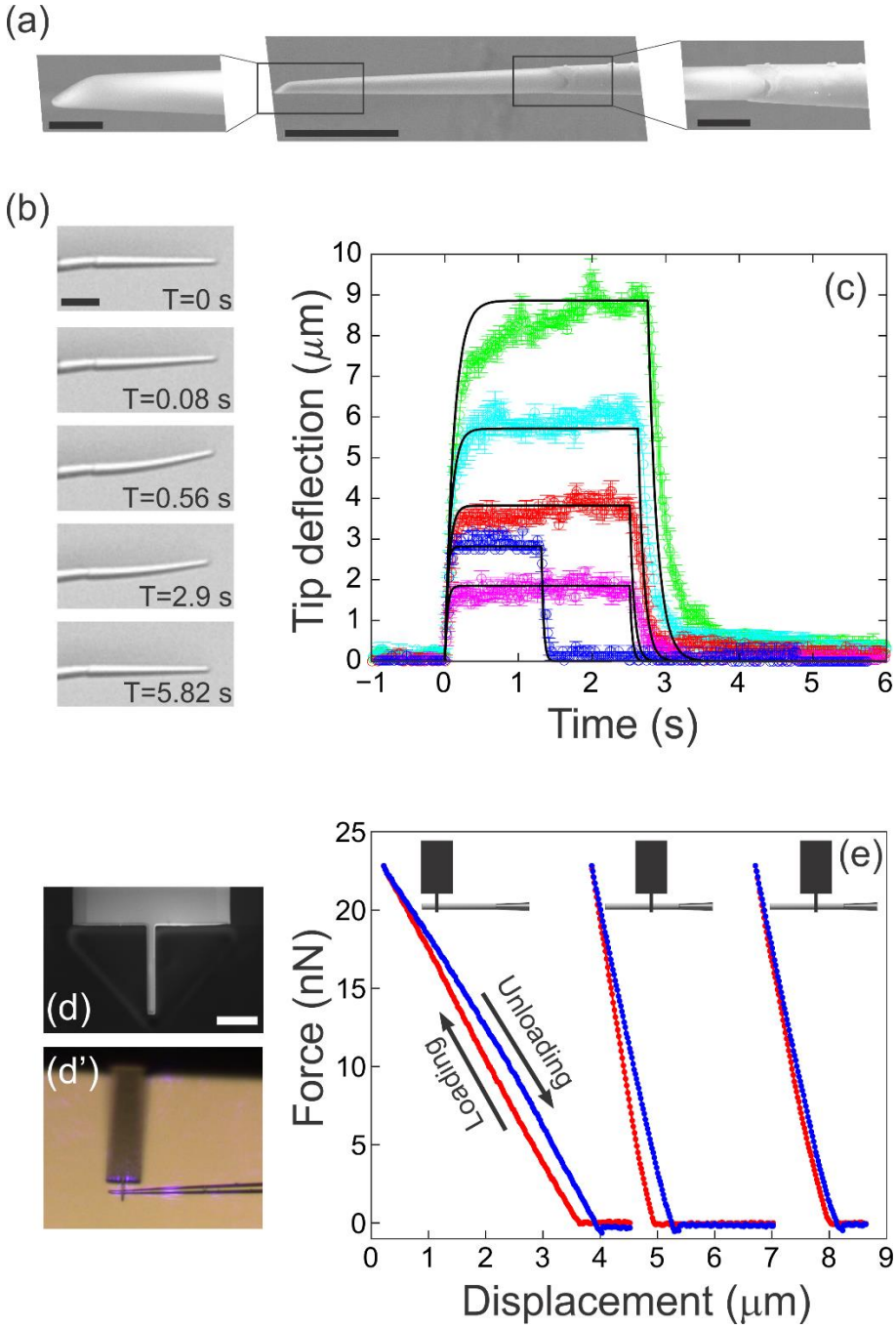

Figure 2. Force calibration. a). SEM image of a typical cantilever. Scale bars are 5, 30 and 10 □m respectively (from left to right). b). Force calibration by dragging the cantilever through a fluid of known viscosity (Tween-20). Different snapshots show the profile of the cantilever at different times. Scalebar: 20 □m. c). Cantilever tip deflection as a function of time for five different cantilevers. d). Commercial AFM cantilever modified to produce a 2 □m thick tip that ensures firm grip between the sample and the probe as well as a precisely defined position of force application. Scalebar: 10 □m. d'). AFM measurement of cantilever stiffness using a probe from d). Violet glare is the laser from the position sensitive detector of the AFM. e). Sample force-displacement obtained from AFM measurements. Red portions of the curves show the loading phase, blue portions correspond to the unloading phase. Initial slope of the loading curve defines the effective spring constant of the cantilever. The two curves on the right are repetitions of the same measurement. Left-most measurement was obtained by applying the force closer to the cantilever tip making the effective spring constant smaller than in the other two measurements (as schematically illustrated in the sketches at the top).

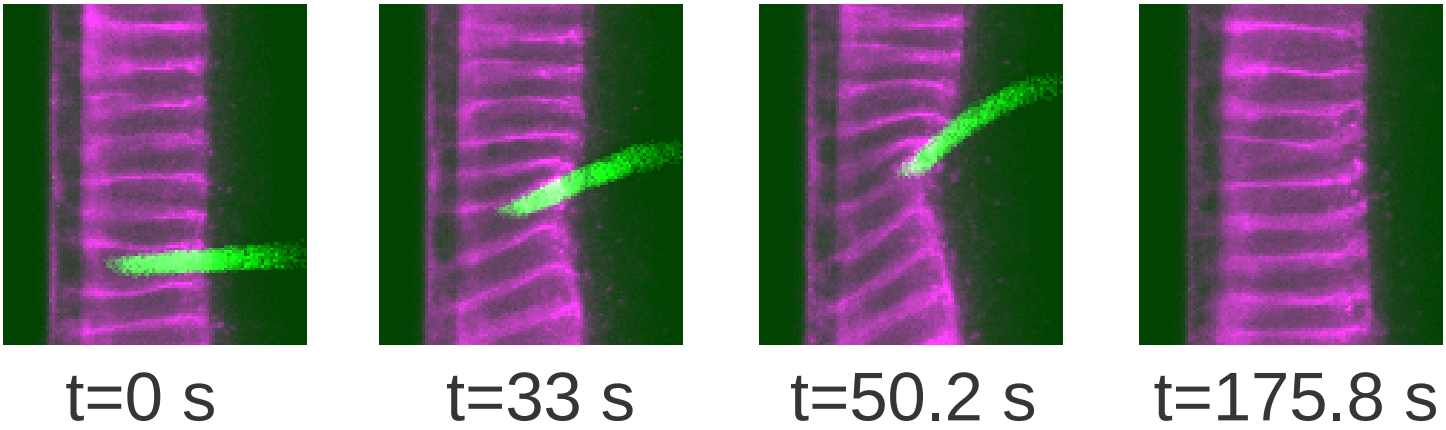

Figure 3. A sample measurement. Cantilever (green) is inserted into one of the cells (magenta) and is pulled upwards. The resulting deflection of the cantilever as well as the deformation of the cellular layer is readily visible and quantifiable. This image was chosen because of a particularly large cantilever deflection. Usually, however, cantilevers used are significantly stiffer such that the deflection is smaller, and the deformation is much more uniform along the thickness of the cellular layer.

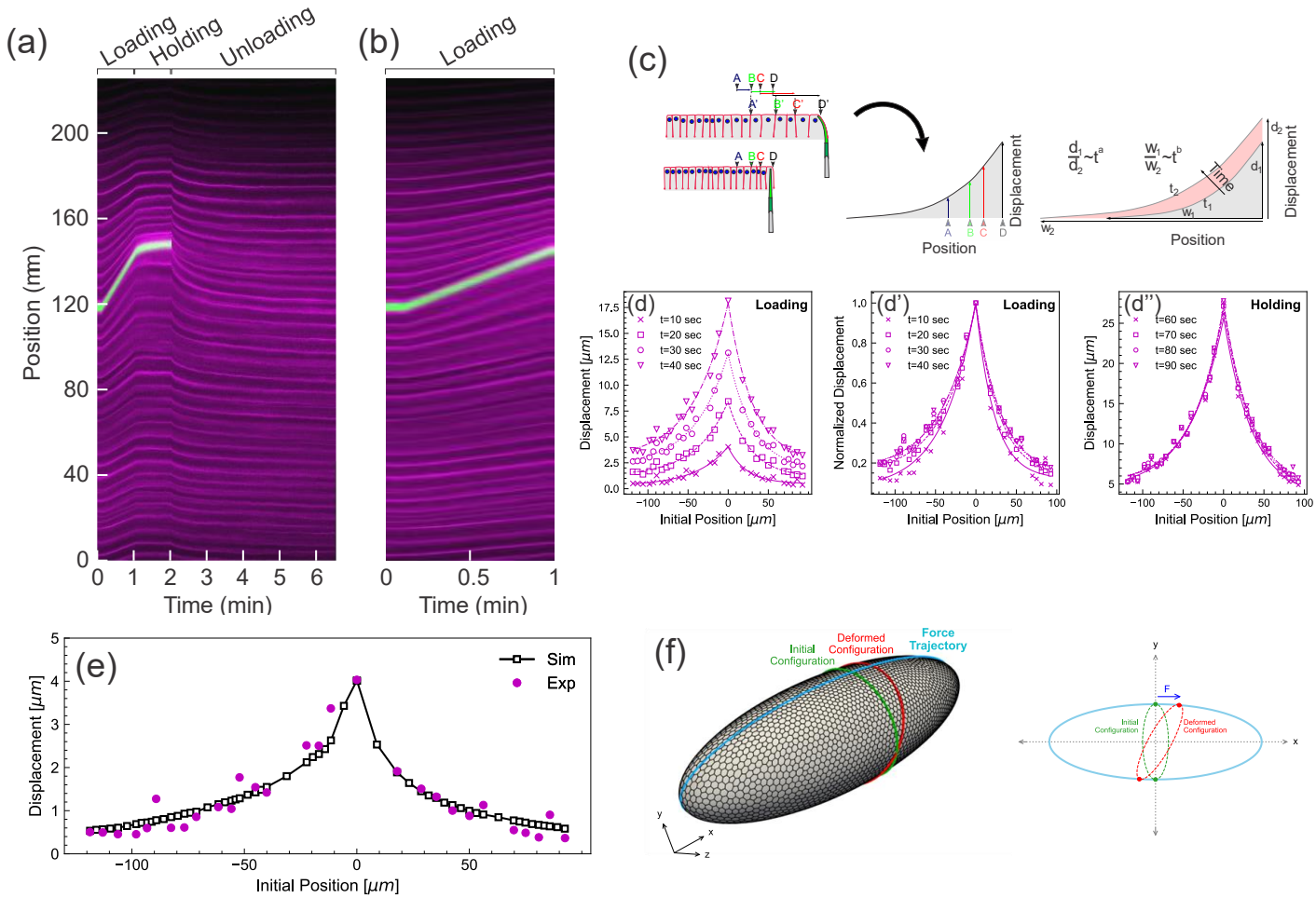

Figure 4. Measurement quantification and analysis. a). Kymograph corresponding to a complete loading-unloading cycle. Green streak corresponds to the cantilever, magenta streaks correspond to the cellular membranes. b). Zoomed in portion of the kymograph from a) showing the loading phase. c). Schematic illustrating how tissue deformation profile is constructed based on the data in the kymograph. d). Time-course of tissue deformation profile (as schematically explained in c)) throughout the course of the loading phase, extracted from the kymograph in a). d'). Same as d), with the curves re-scaled along the y-axis so as to have the same maximum at zero. d''). Time-course of tissue deformation profile in the holding phase. e). Deformation profile measured after 10 s in the loading phase (magenta circles), compared to simulation results (black). Young's modulus of the cellular edges in the simulation was set to 0.00635 nN/mm. f) A schematic explaining how system-size ("boundary") effects may effect the dynamics. A point on the surface of the ellipsoid moving along its surface will cause the corresponding ellipsoid circumference to stretch. Initial configuration of the stretched circumference is shown in green. The same circumference after the tissue is stretched is shown in red.

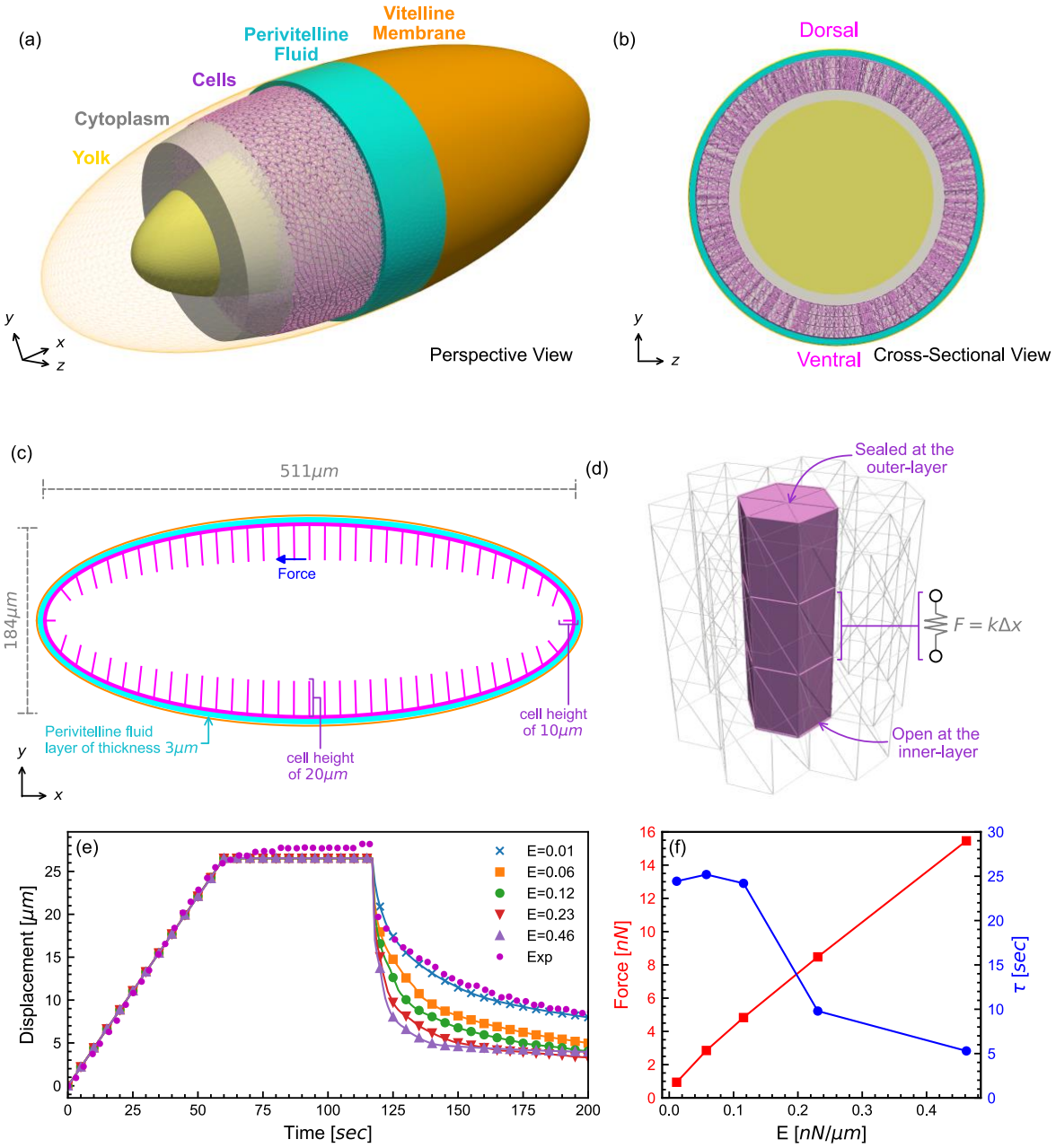

Figure 5. Computational model used to interpret measurement data. a), b). Geometry of a simulated model embryo. An embryo is surrounded by a rigid shell (vitelline membrane) where no-slip boundary is imposed. A thin gap filled with inviscid fluid separates the vitelline membrane from the surface of the embryo (perivitelline space). Cells are prisms whose surfaces are linearly elastic 2D shells. The interior of the embryo (yolk and cytoplasm) is described as Stokes fluid. For details, see text. c). Dimensions of the various inter-embryonic compartments used in the model. d). A model cell is a prism with a linearly elastic surface. e). The displacement of the point where the force is applied as a function of time for varying Young's modulus of cellular edges. f). Quantification of the results in e). The force on the cantilever at the end of loading increases (approximately linearly) with increasing Young's modulus of a cellular edge, whereas the characteristic time of recoil decreases.

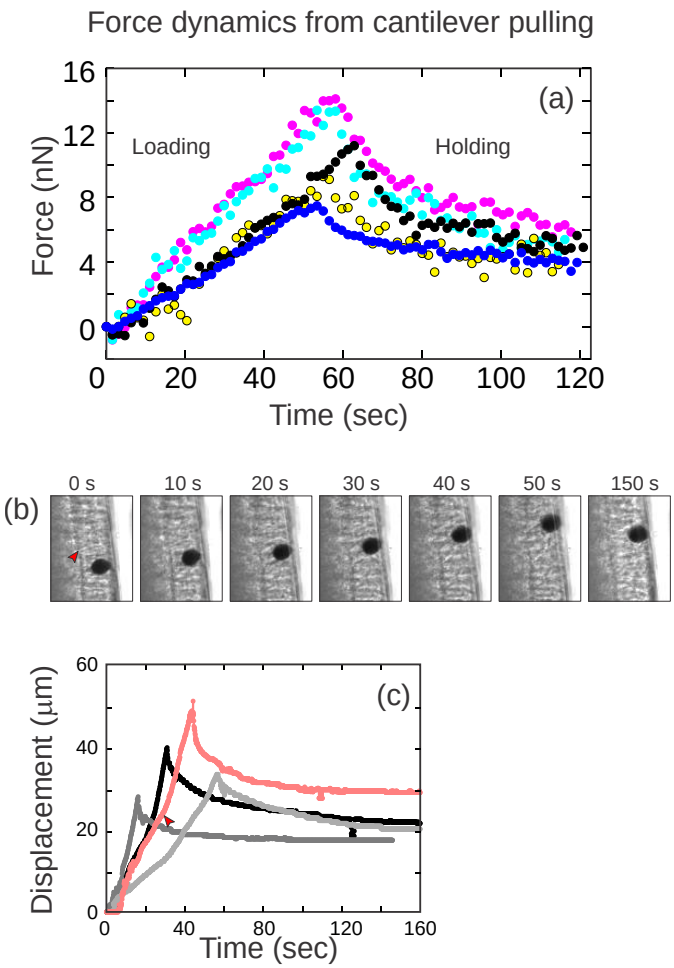

Figure 6. The dynamics of force in a cantilever pulling experiment and ferrofluid-based measurements quantifying the non-uniformity of the material properties along the apico-basal axis of a cell. a). Force on a cantilever as a function of time in five different measurements. b). Ferrofluid pulling experiment. The droplet is pulled towards the magnet and then released after approximately 50 s. Arrowhead indicates the position of the cellularization front (i.e. the basal side of the newly forming cells). c). Ferrofluid droplet displacement measured in four different experiments. Droplets move essentially without slowing down when they don't make contact with the basal side. The curve shown in pink corresponds to a large droplet that made mechanical contact with the basal side in the beginning of pulling. The droplet markedly accelerates as contact with basal side is visibly lost, which happens at the time-point indicated by the red arrowhead.